AIAA JOURNAL
Vol. 35, No. 3, March 1997

Modeling of the Reynolds Stress Transport Equation

L. Djenidi* and R. A. Antonia†
University of Newcastle, Newcastle, New South Wales 2308, Australia

An empirical strategy for improving modeling of the energy dissipation rate ϵ_{ij} and the velocity–pressure gradient Π_{ij} terms in the transport equations for the Reynolds stresses is proposed on the basis of available direct numerical simulations of the turbulent boundary layer and fully developed turbulent channel flow. The dissipation-rate model takes into account the anisotropy of the dissipation rate not only near the wall but elsewhere in the flow as well. When modeling the velocity–pressure gradient term, the usual split between pressure–transport and redistributive terms is avoided. One consequence of this strategy is the elimination of wall reflection or near-wall correction terms. Wall-topography parameters, such as the distance to the wall and wall-normal vectors, are also absent. Calculations of a turbulent boundary layer over a smooth wall confirm the potential improvements that can be achieved with this approach.

I. Introduction

SECOND-MOMENT closures or Reynolds stress models (RSMs) are generally thought to be more reliable than eddy viscosity models (EVMs) for calculating turbulent flows in general and complex turbulent flows in particular.[1] RSMs provide, in principle, greater generality than EVMs because they involve invariant forms.[2] However, to date, none of the existing RSMs is truly universal; consequently, each model needs to be tuned to individual flows. The major problem encountered in development of RSMs relates to how the return-to-isotropy process and the near-wall effects are modeled. In terms of the equations used in any particular RSM, one seeks to model the velocity–pressure gradient correlation Π_{ij}, the dissipation rate tensor ϵ_{ij}, and the turbulent diffusion T_{ij} [see Eq. (1)]. These unknowns are commonly modeled with algebraic equations in terms of second-order moments and mean quantities. T_{ij} is generally smaller than Π_{ij} and ϵ_{ij}, and it is sometimes neglected. It is retained only in particular flow configurations, but even then it appears to have little effect on the results.[3] Most of the existing RSMs adopt a simple model for T_{ij} (Ref. 4). On the other hand, calculation of the Reynolds stresses depends strongly on the way Π_{ij} and ϵ_{ij} are modeled.

The velocity–pressure gradient term has been extensively studied and several models have been proposed. Almost invariably, a common approach has been used. The expression for Π_{ij} is split into a pressure transport term $T_{\pi_{ij}}$ and a redistributive term ϕ_{ij}, which is responsible for the interchange of energy between different Reynolds stress components. Because the former term can be expressed in terms of the triple product of fluctuating velocities,[1] it is incorporated into T_{ij}. The redistributive or pressure-strain term is decomposed into two parts, which are modeled separately (see, for example, Ref. 2). The first part (called linear or rapid part), $\phi_{ij,2}$, responds to a change in the mean velocity gradient, whereas the second part (nonlinear or slow part), $\phi_{ij,1}$, is physically interpreted as a return-to-isotropy. However, although the split of ϕ_{ij} may be convenient,[2] it may not be appropriate, especially near a wall.[5] The turbulent channel flow DNS database[6] seems to suggest that, at low Reynolds numbers, Π_{ij} should be modeled instead of ϕ_{ij}. This is also supported by the DNS database for the canonical turbulent boundary layer.[7]

The second major difficulty relates to the way the average dissipation rate tensor ϵ_{ij} is handled. In most proposals, ϵ_{ij} is assumed to be isotropic—although this is recognized to be incorrect near a solid boundary and a correction is applied in this region, e.g., Ref. 8—of the form $2\epsilon\delta_{ij}/3$, where ϵ ($\equiv \epsilon_{kk}/2$) is the dissipation rate of the turbulent kinetic energy k ($\equiv \overline{u_i u_i}/2$). Departures from isotropy of ϵ_{ij} are often absorbed into the pressure-strain model.[2] Thus, the task of modeling ϵ_{ij} reduces to that of determining ϵ by its own transport equation. Although this method may have been justifiable in the past because of the lack of information about Π_{ij} and ϵ_{ij}, it seems no longer valid, given the availability of the DNS databases. For example, the DNS database for the turbulent boundary layer over a smooth wall[7] shows that Π_{ij} and ϵ_{ij} behave quite differently as the wall is approached. The inclusion of the anisotropy of the dissipation rate in the pressure-strain model seems rather awkward in situations where the anisotropy is relatively important. It would be preferable to model Π_{ij} and ϵ_{ij} separately. This would not only increase the physical correctness of the model but also enhance its generality.

The present paper outlines a possible empirical strategy for developing an RSM for a turbulent boundary layer. Tentative models for Π_{ij} and ϵ_{ij} are developed with the aid of DNS for a turbulent boundary layer[7] and a fully developed turbulent channel flow.[6] The main aim is to eliminate the use of empirical terms, which are commonly introduced to simulate wall effects on the flow (see, for example, Ref. 1). There are basically two reasons for developing an RSM that is free of wall-correction terms. First, such a model would be suitable for calculating flows over nonflat surfaces. Second, it is difficult to devise appropriate wall-correcting terms. The difficulty relates to separating the influence of viscosity from that of wall proximity.[9] The viscosity effect may become significant at low Reynolds numbers even away from a solid boundary. The proximity of a wall imposes a damping effect mainly on the wall-normal fluctuating velocity. Furthermore, all correcting terms invariably use a distance to the wall as well as wall-normal vectors. This makes the models unsuitable for calculating flows over nonflat surfaces—for example, riblet flows.[10] Launder and Li[11] proposed an RSM that does not use wall-topography parameters in the model of ϕ_{ij}. The present approach differs from theirs and allows elimination of wall-topography parameters from the models of ϵ_{ij} and Π_{ij}.

The essential feature of the present strategy is the acknowledgment that there is likely to be a departure from local isotropy in second-order moments of velocity derivatives and ϵ_{ij}. Arguments for abandoning the isotropic model for ϵ_{ij} have been advanced by several authors. According to Reynolds,[12] the dissipation rate tensor shows no tendency to become more isotropic as the Reynolds number increases. By examining the transport equation for ϵ_{ij}, Durbin and Speziale[13] argued that, strictly, local isotropy is not a formally justifiable hypothesis—regardless of the Reynolds number—if the mean rate of strain is not zero. This latter condition is certainly violated near the wall; the channel flow DNS databases suggest that ϵ_{ij} approaches isotropy (without necessarily reaching it) only as the channel centerline is neared.[5] For the boundary layer, the DNS database of Ref. 7 indicates that, even in the outer region, ϵ_{ij} does not reach isotropy.[14] It seems that there is a need to account for this anisotropy to improve the performance of second-moment closures. Accordingly, a nonisotropic form of ϵ_{ij} is proposed (Sec. II.A) on

Received Feb. 3, 1996; revision received Nov. 25, 1996; accepted for publication Dec. 5, 1996; also published in *AIAA Journal on Disc*, Volume 2, Number 2.

*Lecturer, Department of Mechanical Engineering.
†Professor, Department of Mechanical Engineering. Member AIAA.

the basis of DNS databases. These databases suggest that one should model Π_{ij} rather than its components, i.e., the pressure–transport and redistributive terms. Thus, the focus, here, is on Π_{ij} (Sec. II.B). The proposed models for ϵ_{ij} and Π_{ij} are empirical models and, as such, lack mathematical rigor. We believe that this is not too critical because we are mainly concerned with testing new ideas at this stage.

Calculations of a turbulent boundary layer incorporating these models in an RSM are presented and compared (Sec. IV) with experimental and numerical data.

II. Modeling of ϵ_{ij} and Π_{ij}

The transport equations for the Reynolds stresses may be written in shorthand form (e.g., Refs. 5 and 12):

$$(D/Dt)\overline{u_iu_j} = P_{ij} + T_{ij} + D_{ij} + \Pi_{ij} - \epsilon_{ij} \tag{1}$$

where $D/Dt \equiv \partial/\partial t + \bar{U}_k\partial/\partial x_k$ and the terms on the right-hand side are as follows (the notation is essentially that of Ref. 5):

$$P_{ij} = -(\overline{u_iu_k}\bar{U}_{j,k} + \overline{u_ju_k}\bar{U}_{i,k}) \qquad T_{ij} = -(\overline{u_iu_ju_k})_{,k}$$

$$D_{ij} = (\overline{u_iu_j})_{,kk} \qquad \Pi_{ij} = -(\overline{u_ip_{,j} + u_jp_{,i}})$$

$$\epsilon_{ij} = 2\overline{u_{i,k}u_{j,k}}$$

P_{ij} is the production rate, T_{ij} is the turbulent transport rate, D_{ij} is the viscous diffusion rate, Π_{ij} is the velocity–pressure gradient term, and ϵ_{ij} is the dissipation rate.

For reasons discussed earlier, we concentrate only on Π_{ij} and ϵ_{ij}, noting that P_{ij} and D_{ij} do not require modeling. A simple form for T_{ij} (Ref. 4) is used in the present work:

$$T_{ij} = \left[C_s(k/\epsilon)\overline{u_ku_\ell}(\overline{u_iu_j})_{,\ell}\right]_{,k}$$

where $C_s = 0.22$.

A. ϵ_{ij}

Most of the current models for this term are of the form

$$\epsilon_{ij} = f_\epsilon(\epsilon_{ij})_{nw} + (1 - f_\epsilon)(\epsilon_{ij})_0 \tag{2}$$

where $(\epsilon_{ij})_{nw}$ and $(\epsilon_{ij})_0$ are models of ϵ_{ij} that apply within and outside the near-wall region, respectively, and f_ϵ represents a weighting function that is equal to 1 near the wall and zero a short distance away from the wall.

The form of $(\epsilon_{ij})_{nw}$ should satisfy the limiting wall behavior of the dissipation rate tensor.[8]

Launder and Tselepidakis[3] proposed the following, tensorially correct, model for $(\epsilon_{ij})_{nw}$:

$$(\epsilon_{ij})_{nw} = \frac{\epsilon}{k}\frac{\overline{u_iu_j} + \overline{u_iu_k}n_jn_k + \overline{u_ju_k}n_in_k + n_in_j\overline{u_ku_\ell}n_kn_\ell}{1 + \frac{3}{2}(\overline{u_pu_q}/k)n_pn_q} \tag{3}$$

where n_k is the unit vector (0, 1, 0) normal to the wall. Expression (3) satisfies the correct asymptotic behavior[8] (in the limit $y \to 0$) and contracts properly ($\epsilon_{ij} = 2\epsilon$ when $i = j$. Equation (3) has also been used by Lai and So,[15] with f_ϵ (or $f_{w,1}$ in their notation) given by

$$f_\epsilon = \exp\left[-(R_T/150)^2\right] \tag{4}$$

where $R_T = k^2/\nu\epsilon$ is a turbulence Reynolds number. Launder and Tselepidakis[3] avoid R_T, using instead

$$f_\epsilon = \exp(-20A_b^2) \tag{5}$$

where $A_b \equiv 1 + 9(II_b + 3III_b)$. II_b ($\equiv -b_{ik}b_{ki}/2$) and III_b ($\equiv b_{ik}b_{k\ell}b_{\ell i}/3$) are the second and third invariants of the Reynolds stress anisotropy tensor $b_{ij} \equiv \overline{u_iu_j}/2k - \delta_j/3$ (the notation is the same as in Ref. 2). As the wall is approached, the turbulence tends toward a two-component state ($\overline{v^2}$ is much smaller than $\overline{u^2}$ or $\overline{w^2}$) and the invariants tend to satisfy the relation $\frac{1}{9} + 3III + II = 0$ (i.e., the upper boundary on the anisotropy invariant map).[16] It follows that A_b (Launder and Tselepidakis[3] refer to it as a flatness parameter) approaches zero so that $f_\epsilon \to 0$, as required by the formulation in Ref. 2. Launder and Tselepidakis (see also Ref. 9) suggested that it may be desirable to consider invariants of the stress dissipation-rate tensor. If the dissipation-rate anisotropy tensor is denoted by d_{ij}, where

$$d_{ij} = (\epsilon_{ij}/2\epsilon) - (\delta_{ij}/3) \tag{6}$$

a parameter $A_d \equiv 1 + 9(II_d + 3III_d)$, with $II_d \equiv -d_{ik}d_{ki}/2$ and $III_d \equiv d_{ik}d_{k\ell}d_{\ell i}/3$, can be introduced in similar fashion to A_b.

For $(\epsilon_{ij})_0$, a relatively standard approach is to assume (local) isotropy for ϵ_{ij}, namely,

$$(\epsilon_{ij})_0 = \tfrac{2}{3}\epsilon\delta_{ij} \tag{7}$$

As noted in the Introduction, there does not seem to be any evidence—either experimental or based on the DNS data—in support of (7). Even at the centerline of the channel, ϵ_{ij} exhibits a small but discernible departure from isotropy (e.g., Ref. 17). The DNS data of Spalart[7] indicate (see Ref. 14) that, in the outer region of the boundary layer, although the magnitudes of II_d and III_d decrease as the Reynolds number increases they do not vanish at the highest Reynolds number of the simulation ($R_\theta = 1410$). Reynolds[12] observed the same trend from the DNS data of Rogallo (reference given in Ref. 12). Mansour et al.[5] noted that the relation

$$d_{ij} = b_{ij} \tag{8}$$

provides better agreement with the DNS channel flow data of Kim et al.[6] than dissipation-rate models that use (7). Mansour et al.[5] pointed to the similarity between invariant maps of d_{ij} and b_{ij} as support for (8). Cross plots (not shown here) of d_{ij} vs b_{ij} (for $i \equiv j = 1, 2, 3$), based on both boundary layer (see Ref. 14) and channel flow DNS data, show that, outside the near-wall region, the general trend may be roughly approximated by

$$d_{ij} = \alpha b_{ij} \qquad (i \equiv j = 1, 2, 3) \tag{9a}$$

which may be thought of as a linear approximation to the nonlinear algebraic model for ϵ_{ij} (expressed in terms of b_{ij}) developed by Hallbäck et al.[18] Strictly, the constant of proportionality should depend on the Reynolds number, preferably a local Reynolds number such as R_T (α may depend on other parameters). Using scaling arguments similar to those used by Tennekes and Lumley[19] and Lumley,[20] Antonia et al.[14] obtained

$$d_{ij} = 10R_T^{-\frac{1}{2}}b_{ij} \qquad (i \equiv j = 1, 2, 3) \tag{9b}$$

Equation (9b) is not satisfactory near the channel centerline or the edge of the boundary layer; nor do they apply in the near-wall region. Because as $y \to 0$, Eq. (8) becomes more appropriate at least for $i = j = 1$ and $i = j = 3$, the form

$$d_{ij} = \alpha_{R_T}b_{ij} \tag{9c}$$

where $\alpha_{R_T} = \min(1, 10R_T^{-1/2})$ is used in the present calculations. In light of these observations, the following model is suggested for ϵ_{ij}:

$$\epsilon_{ij} = 2\epsilon\left[\alpha_{R_T}b_{ij} + (\delta_{ij}/3)\right] \tag{10}$$

This form has two interesting features: 1) it is valid throughout the layer and 2) it thus avoids the use of a rather arbitrary bridging function between inner and outer regions. Note also the elimination of the wall-normal vector, which should, in principle, make the model suitable for nonplanar surfaces. On the other hand, it gives an incorrect limiting behavior for ϵ_{22} at the wall ($\epsilon_{22} = \epsilon/k\overline{u_2^2}$ instead of $4\epsilon/k\overline{u_2^2}$). This, however, should not be too critical from a calculation viewpoint because ϵ_{22} satisfies the limiting behavior only when y^+ is very small ($y^+ < 1$), a region mainly governed by viscosity. In any case, trying to enforce the asymptotic wall behavior at the expense of obtaining only approximate results away from the wall seems unwarranted. Also, formulation (2) can be used if necessary; for example, in the present case (see Ref. 14),

$$\epsilon_{ij} = f_\epsilon(\epsilon_{ij})_{nw} + 2\epsilon(1 - f_\epsilon)\left[10R_T^{-\frac{1}{2}}b_{ij} + (\delta_{ij}/3)\right] \tag{11}$$

Distributions obtained with Eq. (10) compare relatively well with the boundary layer DNS data (Fig. 1). The DNS data of Ref. 7 ($R_\theta = 1410$) have been used in this figure and all subsequent figures for

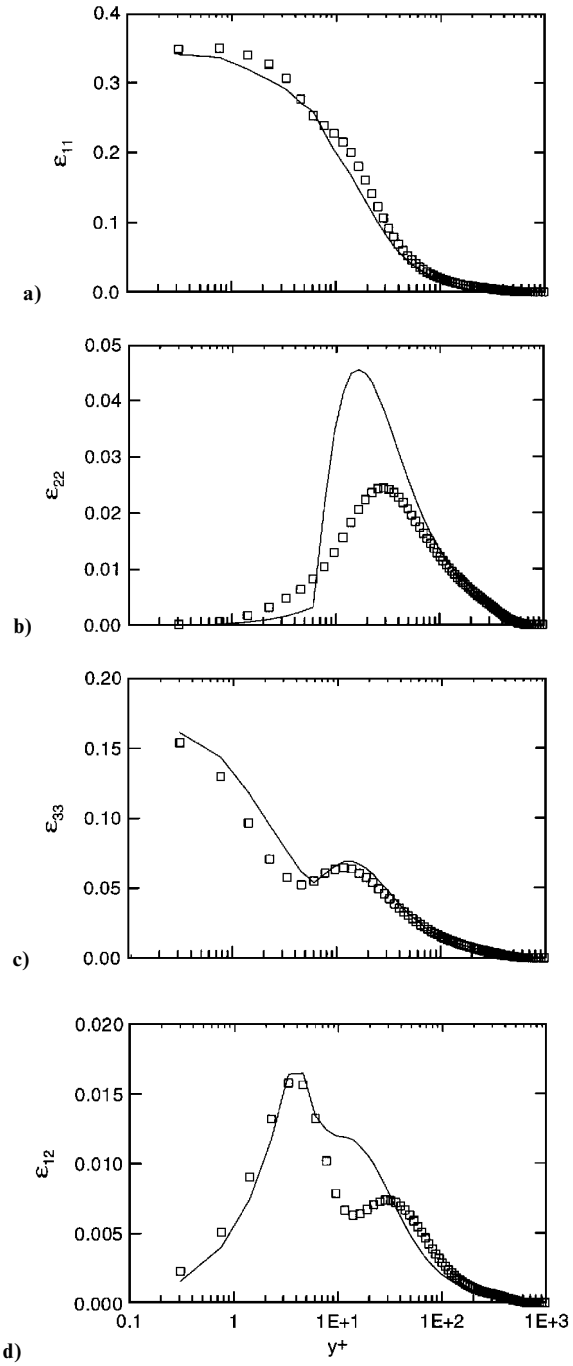

Fig. 1 Four components of the dissipation rate tensor (R_θ = 1410): ——, present model [Eq. (11)] and □, DNS (from Ref. 7).

developing models of ϵ_{ij} and Π_{ij}. Note, however, that the near-wall model of ϵ_{ij} (particularly when $i \equiv j = 2$) needs to be improved.

Equation (10) applies only for $i = j = 1, 2, 3$; it does not, in principle, apply for $i = 1$, $j = 2$. However, Fig. 1d indicates that Eq. (10) provides a reasonably good approximation for ϵ_{12} when $\alpha_{R_T} = \min(2, 10R_T^{-1/2})$. Although the use of different values of α_{R_T} in the near-wall region (i.e., 1 for the diagonal terms of dissipation tensor and 2 for ϵ_{12}) is arguably not justifiable, the motivation was to obtain a correct limiting behavior of ϵ_{12} at the wall. Furthermore, calculations using the near-wall value of 1 for α_{R_T} for all the components of ϵ_{ij} did not produce noticeable differences in the results. This is of interest because the model should be relevant to nonplanar surface flows, given the scalar value of α_{R_T}.

B. Π_{ij}

Model for Π_{ij}

The DNS channel data[5] suggest that one should model Π_{ij} rather than its components (the pressure–transport and redistributive term). Thus, the focus here is on Π_{ij} and the approach is much more empirical than mathematical. The starting point is the transport equation for b_{ij}:

$$\frac{D}{Dt}b_{ij} = \frac{1}{k}\left[\left(P_{ij} - \frac{\overline{u_iu_j}}{2k}P_{kk}\right) + \left(\Pi_{ij} - \frac{\overline{u_iu_j}}{2k}\Pi_{kk}\right) - \left(\epsilon_{ij} - \frac{\overline{u_iu_j}}{2k}\epsilon_{kk}\right)\right] \tag{12}$$

where the viscous and turbulent diffusion terms have been neglected. Because Π_{kk} is almost zero in the outer region of the flow (see Refs. 5 and 7), the term $[\Pi_{ij} - (\overline{u_iu_j}/2k)\Pi_{kk}]$ can be assimilated with Π_{ij}. As a first step toward a more elaborate model, Π_{ij} is modeled as follows:

$$\Pi_{ij} = c_1\left(\epsilon_{ij} - \frac{\overline{u_iu_j}}{2k}\epsilon_{kk}\right) - c_2\left(P_{ij} - \frac{\overline{u_iu_j}}{2k}P_{kk}\right) \tag{13a}$$

Equation (13a) can be rewritten in the following form:

$$\Pi_{ij} = -C_1\epsilon b_{ij} + C_1'\epsilon d_{ij} - C_2(P_{ij} - \tfrac{1}{3}\delta_{ij}P_{kk}) + C_2'b_{ij}P_{kk} \tag{13b}$$

The first and second terms on the right-hand side of Eq. (13b) are identified with the slow part (or return-to-isotropy), and the third and fourth terms are identified with the rapid part. These parts will be symbolically represented as $\Pi_{ij,1}$ and $\Pi_{ij,2}$, respectively. $\Pi_{ij,1}$ reduces to Rotta's[21] model when $C_1' = 0$ (i.e., local isotropy), and $\Pi_{ij,2}$ reduces to Launder et al.'s[22] [isotropization-of-production (IP)] model if $C_2' = 0$.

Analysis of the Model

The present formulation for $\Pi_{ij,1}$ recognizes that the components of the turbulent energy dissipation rate may not satisfy isotropy (i.e., $\epsilon_{ij} \neq \frac{2}{3}\delta_{ij}\epsilon$); the latter would be especially true in the near-wall region. This is an important departure from the standard approach for modeling the return-to-isotropy (e.g., Ref. 12). Arguing that differences observed between experiments and calculations based on Rotta's model are due to differences in the structure of small-scale turbulence, Reynolds[12] conjectured that b_{ij} and d_{ij} should be coupled and suggested that d_{ij} would assist b_{ij} in returning to isotropy. We observe that the present form of $\Pi_{ij,1}$, namely,

$$\Pi_{ij,1} = C_1\epsilon b_{ij} + C_1'\epsilon d_{ij} \tag{14a}$$

is consistent with this process.

Classically, the return-to-isotropy term is improved by adding nonlinear terms in Rotta's model (see, for example, Ref. 2). Such a procedure assumes that the observed discrepancies between experiments and Rotta's model are due to effects that are nonlinear in b_{ij}. It could also be that the nonisotropic character of the small-scale structures causes the return-to-isotropy not to be correctly reproduced in b_{ij} only. The dissipation tensor d_{ij} may well be included in any attempt to model the return-to-isotropy process. This is supported by the fact that d_{ij} can be of comparable magnitude to b_{ij} (see Ref. 14). Note that, from a modeling point of view, nonlinear (as well as linear) terms in b_{ij} can be introduced in the expression for $\Pi_{ij,1}$ through the modeling of d_{ij} [Eqs. (10) in Ref. 14]. Substitution of Eq. (9c) for d_{ij} in Eq. (14a) yields

$$\Pi_{ij,1} = -(C_1 - C_1'\alpha_{R_T})\epsilon b_{ij} \tag{14b}$$

The expression for the rapid part $\Pi_{ij,2}$, i.e.,

$$\Pi_{ij,2} = -C_2(P_{ij} - \tfrac{1}{3}\delta_{ij}P_{kk}) + C_2'b_{ij}P_{kk} \tag{15a}$$

can be recast into the form

$$\Pi_{ij,2} = k\left[C_2\tfrac{2}{3}S_{ij} + C_3(b_{ik}S_{jk} + b_{jk}S_{ik} - \tfrac{2}{3}\delta_{ij}b_{kl}S_{kl}) + C_4(b_{ik}\Omega_{jk} + b_{jk}\Omega_{ik}) + C_5b_{ij}b_{kl}S_{kl}\right] \tag{15b}$$

where

$$S_{ij} = \frac{1}{2}\left(\frac{\partial\bar{U}_i}{\partial x_j} + \frac{\partial\bar{U}_j}{\partial x_i}\right) \quad \text{and} \quad \Omega_{ij} = \frac{1}{2}\left(\frac{\partial\bar{U}_i}{\partial x_j} - \frac{\partial\bar{U}_j}{\partial x_i}\right)$$

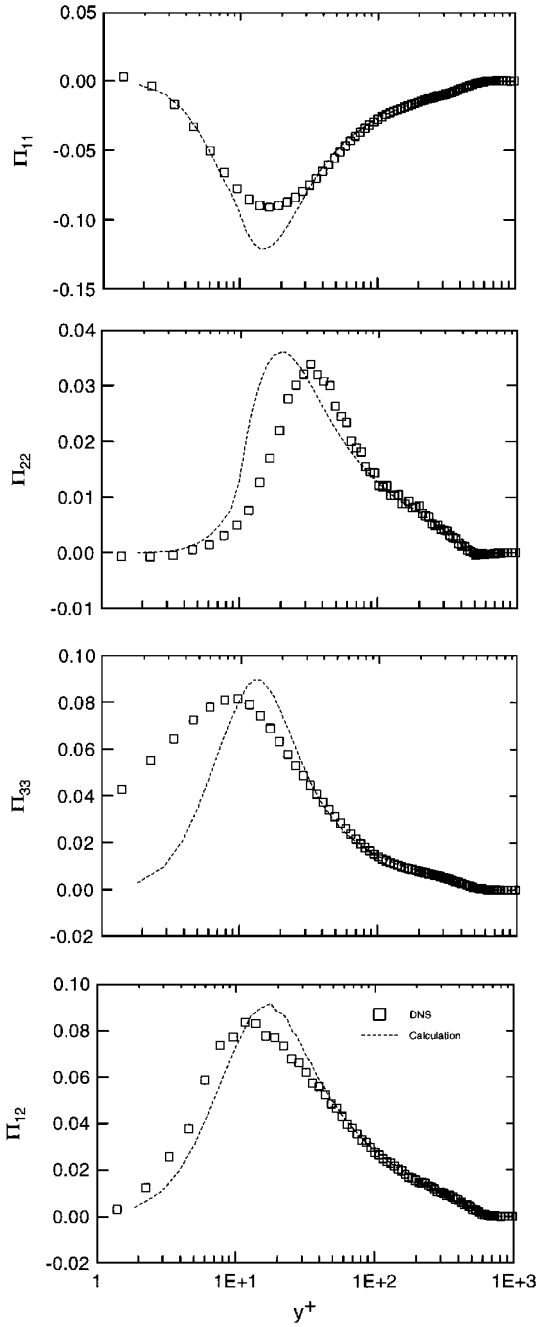

Fig. 2 Four components of the velocity–pressure gradient tensor (R_θ = 1414): ——, present model [Eq. (20)] and □, DNS (from Ref. 7).

This expression bears a resemblance to $\phi_{ij,2}$, where terms that are cubic in b_{ij} have been neglected (see, for example, Refs. 5 and 9). For the present study, however, (15a) is preferred to (15b). The former expression is equivalent to that for $\phi_{ij,2}$ developed by Launder[23] when only the first and second terms are considered.

Substituting the forms (14b) and (15a) into the transport equations for the Reynolds stresses [Eq. (1)], one finds that the two-component limit constraint is satisfied when $C_1 = C_1'(=1)$. The realizability condition ($u_i = 0$ leads to $D\overline{u_i u_i}/Dt = 0$, no summation on i) is also satisfied for the present type of calculation (boundary layer flow). Thus, the final form for Π_{ij} is

$$\Pi_{ij} = -C_1(1 - \alpha_{R_T})\epsilon b_{ij} - C_2(P_{ij} - \tfrac{1}{3}\delta_{ij}P_{kk}) + C_2' b_{ij} P_{kk} \quad (16)$$

This form satisfies symmetry and continuity conditions.

Figure 2 compares the distributions of Π_{ij} calculated with Eq. (16) (where $C_1 = 1$ and $C_2 = C_2' = 1$) and Π_{ij}^{DNS} [where $\Pi_{ij}^{\mathrm{DNS}} = -\overline{(u_i p_{,j} + u_j p_{,i})}$ is obtained from the DNS Reynolds stress budgets of Ref. 7]. There is generally good agreement between Π_{ij} and Π_{ij}^{DNS}

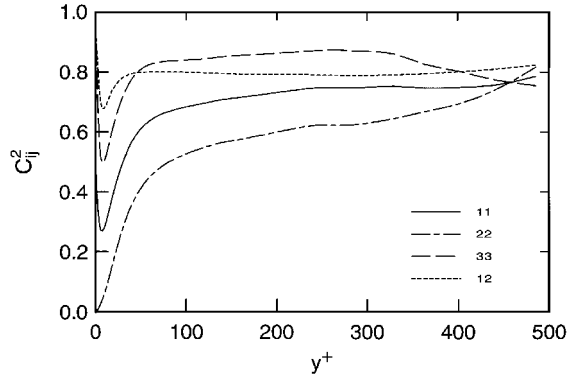

Fig. 3 Coefficients C_2^{ij} in Eq. (21).

for $y^+ \gtrsim 40$ ($y^+ \gtrsim 80$ when $i = j = 2$). Note that, although it is not meant to work in the near-wall region, the model reproduces the trend (except when $i = j = 3$) of the DNS data in that region. Note also that the asymptotic behavior of Π_{ij} as $y^+ \to 0$ is in reasonable agreement with that exhibited by the DNS data, except for $i = j = 3$. This indicates that, although empirical, (16) is a potential candidate to model Π_{ij} throughout the layer. In that case, there would be no need to introduce (near-wall) correcting terms and the model should be suitable for nonplanar surfaces. However, it was found that calculations with $C_2 = C_2' = 1$ did not yield reasonable results when the Reynolds number changed significantly between inlet and outlet conditions. In that case, new values for C_2 and C_2' would be needed.

From a numerical point of view, it is worthwhile comparing (15a) with the IP model for $\phi_{ij,2}$. Matching the form (15a) (where $C_2 = C_2' = 1$) with the IP model implies that the coefficient in the latter model can be defined as

$$C_2^{ij} = 1 - \frac{b_{ij} P_{kk}}{P_{ij} - \frac{1}{3}\delta_{ij} P_{kk}} \quad (17)$$

It is important not to confuse the scalar C_2^{ij} with a tensor C_{ij}^2; C_2^{ij} is a scalar whose numerical value changes with the Reynolds stress components. Figure 3 shows plots of C_2^{ij} for $i = j = 1, 2, 3$ and $i = 1$, $j = 2$. C_2^{ij} has a nearly constant value across the layer [near-wall values of C_2^{ij} are meaningless because (15a) is, in principle, not valid in that region]; but it differs for different Reynolds stress components.

For the present purpose, it seems reasonable to model $\Pi_{ij,2}$ as

$$\Pi_{ij,2} = -C_2^{ij}(P_{ij} - \tfrac{1}{3}\delta_{ij} P_{kk}) + C_2'^{ij} b_{ij} P_{kk} \quad (18)$$

where the values of C_2^{ij} are deduced from Fig. 4. $C_2'^{ij}$ is determined in Sec. IV.

III. Assessment of the Proposed Models of ϵ_{ij} and Π_{ij}

The proposed models of ϵ_{ij} and Π_{ij} rest on empirical arguments based on DNS data only. It is clear that the outlined strategy developed here lacks mathematical rigor and the models are not tensorially invariant. In that respect, the present models for ϵ_{ij} and Π_{ij} can be taken only as suggestions, which, we believe, are worth testing. To this end, we assess whether the models are suitable for calculating a turbulent boundary layer over a smooth wall.

A. Boundary and Initial Conditions: Numerical Method

The present models for ϵ_{ij} and Π_{ij} were introduced in an RSM to calculate a zero-pressure gradient, two-dimensional turbulent boundary layer. The equations of conservation of mass and streamwise momentum are

$$\frac{\partial \bar{U}}{\partial x} + \frac{\partial \bar{V}}{\partial y} = 0 \quad (19)$$

$$\bar{U}\frac{\partial \bar{U}}{\partial x} + \bar{V}\frac{\partial \bar{U}}{\partial y} = \nu\frac{\partial^2 \bar{U}}{\partial y^2} + \frac{\partial(-\overline{uv})}{\partial y} \quad (20)$$

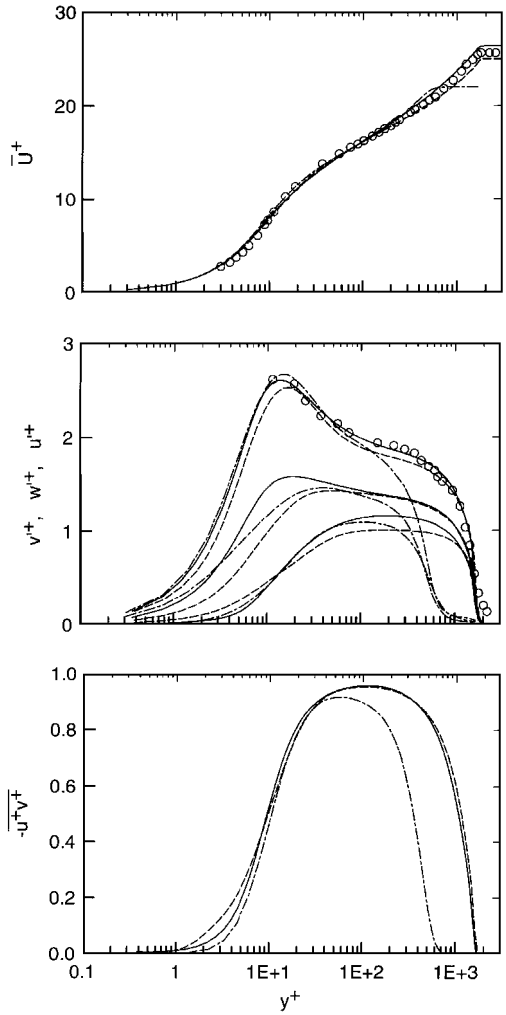

Fig. 4 Mean velocity and Reynolds stress distributions: ——, present model R_θ = 5100; – – –, Launder and Shima's[26] model; and – · –, DNS (from Ref. 7, R_θ = 1410).

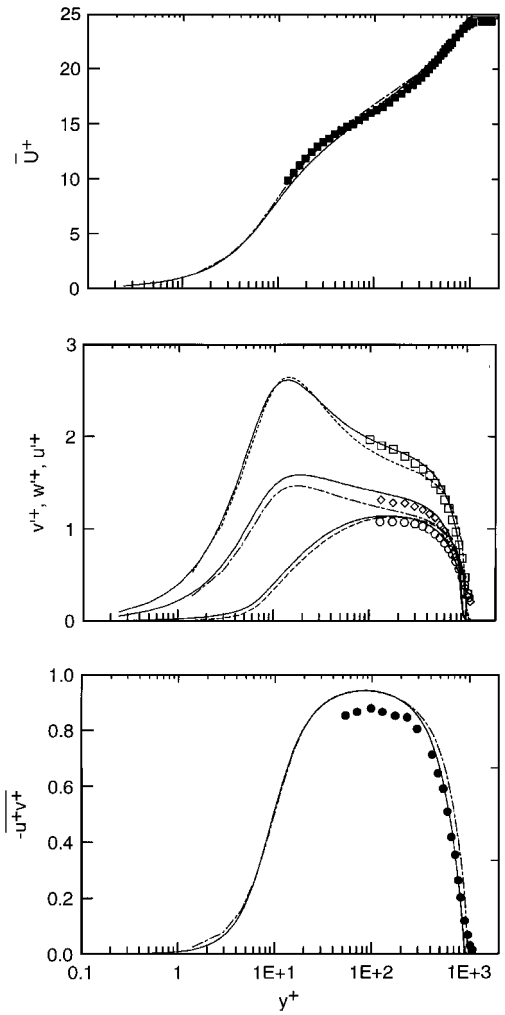

Fig. 5 Mean velocity and Reynolds stress distributions (R_θ = 2800): broken lines, calculations with $C_2 = \frac{1}{4}(C_2^{11} + C_2^{22} + C_2^{33} + C_2^{12})$; solid lines, calculations with C_2^{ij}; and symbols, experimental results of Erm.[30]

The boundary conditions are $\bar{U}_i = \overline{u_i u_j} = 0$ and $\partial\epsilon/\partial y = 0$—although not strictly correct, $\partial\epsilon/\partial y = 0$ was preferred to $\epsilon_w = 2\nu(\partial k^{1/2}/\partial y)^2$ to reinforce numerical stability—at the wall; $\partial\bar{U}_i/\partial y = \partial\overline{u_i u_j}/\partial y = \partial\epsilon/\partial y = 0$ at distance $y > \delta$ (δ is the boundary layer thickness). The DNS[8] data for $\bar{U}$, $\overline{u_i u_j}$, and ϵ at $R_\theta = 670$ were used as initial distributions to start the computations. A control finite volume procedure is used for the discretization of Eqs. (1), (19), and (20) based on an orthogonal mesh and a staggered grid. The solution procedure is an x-marching method, where the finite volume scheme was used at each step in the x direction. The discretized system was solved with the modified strongly implicit algorithm of Schneider and Zedan[24]; 140 nodes were used across the layer with a substantial proportion of these points in the region $y^+ \lesssim 10$; the first node was at about $y^+ = 0.2$.

B. Results

For clarity, we summarize the models for ϵ_{ij} and Π_{ij} developed in the previous sections:

$$\epsilon_{ij} = 2\epsilon\left[\alpha_{R_T} b_{ij} + (\delta_{ij}/3)\right] \tag{21}$$

$$\Pi_{ij} = -C_1(1 - \alpha_{R_T})\epsilon b_{ij} - C_2^{ij}(P_{ij} - \tfrac{1}{3}\delta_{ij} P_{kk}) + C_2^{ij} b_{ij} P_{kk} \tag{22}$$

where

$$\alpha_{R_T} = \begin{cases} \min\left(1, 10 R_T^{-\frac{1}{2}}\right) & (i \equiv j = 1, 2, 3) \\ \min\left(2, 10 R_T^{-\frac{1}{2}}\right) & (i = 1, j = 2) \end{cases}$$

$C_1 = 1$, $C_2^{11} = 0.73$, $C_2^{22} = 0.65$, $C_2^{33} = 0.85$, and $C_2^{12} = 0.79$. Calibration of the model for Π_{ij} with the DNS data of Ref. 7 produced

$$C_2^{ij} = C_2^{ij}\sqrt{A_b}\exp[-(0.0067 R_T)^2]$$

Preliminary calculations showed that the magnitudes of C_1, C_2^{11}, and C_2^{22} should decrease in the near-wall region to reduce the level of Π_{ij}; this was achieved with the use of the function $f_{R_T} = 1 - \exp[-(0.0067 R_T)^2]$; for C_2^{22}, $f_{R_T} = 1 - \exp[-(0.004 R_T)^2]$.

The turbulent kinetic energy dissipation rate was taken from the ϵ equation of Kawamura.[25]

Turbulent Boundary Layer on a Flat Plate

The main objective here is to ascertain whether models (21) and (22), empirically developed, can produce reasonable results, particularly in the near-wall region. The calculated mean velocity and Reynolds stress distributions are compared in Fig. 4 with those obtained by Launder and Shima's[26] model and the experimental data of Purtell et al.[27] ($R_\theta = 5100$). Calculations with our present model follow both Launder and Shima's[26] and Purtell et al.'s[27] data quite closely.

To ascertain the near-wall region calculation, we included the DNS data of Ref. 7 at $R_\theta = 1410$. The comparison between data at $R_\theta = 5100$ and 1410 should be treated with caution because of low Reynolds number effects, which extend well into the sublayer.[28] However, in the sublayer, these effects are less significant between $R_\theta = 1410$ and 5100 than those observed when R_θ varies between 300 and 1410. In this context, the agreement between our present

calculation and the DNS data in the near-wall region seems reasonable. This is rather encouraging because no near-wall correcting terms have been introduced in the present calculation. Generally, the calculated near-wall distributions of the Reynolds stresses reproduce the DNS data fairly well. Only when $i \equiv j = 3$ do our calculated Reynolds stresses show significant discrepancies in the region $3 \lesssim y^+ \lesssim 25$. These discrepancies can be reduced if the coefficient C_2^{33} is reduced in the same way as C_2^{11} and C_2^{22}. This, however, causes the limiting behavior of $\overline{w^2}$ to depart from that in the DNS data as $y^+ \longrightarrow 0$.

It can be argued that because the value of the coefficient C_2^{ij} changes with the Reynolds stress components, the model of Π_{ij} is dependent on the wall geometry or the system of the coordinates used. To remedy this defect two options are available: one can either develop a tensor form for C_2^{ij} or reduce it to a true scalar, that is, C_2^{ij} must be independent of all combinations of i and j. For the present purpose, the second solution is sufficient. Because the values of C_2^{ij} do not show significant differences, C_2 is approximated as follows:

$$C_2 = \tfrac{1}{4}(C_2^{11} + C_2^{22} + C_2^{33} + C_2^{12})$$

This yields $C_2 = 0.755$. This approach, previously used by Tavoularis and Karnik,[29] contrasts with the more common one (see, for example, Ref. 8) for determining C_2 in the model of ϕ_{ij}. The results of the calculation ($R_\theta = 2800$) are compared in Fig. 5 with Erm's[30] data at the same R_θ. Clearly, there are no major changes relative to the previous results. It is plausible that an optimum value of C_2, which minimizes these changes, could be found by trial and error.

IV. Concluding Remarks

An empirical strategy for developing an RSM for boundary layers has been outlined and applied on the basis of available direct numerical simulations of a turbulent boundary layer and a fully developed turbulent channel flow. The main focus is on the dissipation rate ϵ_{ij} and velocity–pressure gradient Π_{ij} terms of the Reynolds stress transport equations. Intrinsic in this strategy is recognition of a departure from local isotropy when modeling ϵ_{ij} and Π_{ij}.

A feature of the proposed model for ϵ_{ij} is that the anisotropy of ϵ_{ij} is taken into account not only in the near-wall region but everywhere in the layer. This feature was also used in modeling Π_{ij}, where the usual split into pressure–transport and redistributive terms is avoided. Neither near-wall correction terms nor wall-topography parameters such as the normal-to-the-wall distance and wall-normal vectors are used. RSMs that incorporate these features should, in principle, be suitable for calculating nonplanar surface flows and therefore represent a significant improvement over current RSMs for near-wall turbulence calculations.

The present models for ϵ_{ij} and Π_{ij} have been included in an RSM to calculate turbulent boundary layers over a smooth surface. The calculated mean velocity and Reynolds stress distributions compare well with those calculated with an existing RSM and experimental data. Also the near-wall behavior of these quantities is in general agreement with the DNS data. In particular, the wall-blocking effect on the wall-normal component of the velocity fluctuation is well captured. This is encouraging considering that there is no near-wall correction term in the Π_{ij} model.

More generally, the present study shows that, aside from elimination of arbitary near-wall correction terms, new, albeit ad hoc, strategies in turbulence modeling are possible. We recognize, however, that the present proposals for ϵ_{ij} and Π_{ij} lack generality and mathematical rigor; as such, they should be treated only as a first step toward more improved modeling.

Acknowledgment

The support of the Australian Research Council is gratefully acknowledged.

References

[1]Launder, B. E., "Second-Moment Closure: Present and Future?" *International Journal of Heat and Fluid Flow*, Vol. 10, No. 4, 1989, pp. 282–300.

[2]Lumley, J. L., "Computational Modeling of Turbulent Flows," *Advances in Applied Mechanics*, Vol. 18, 1978, pp. 123–176.

[3]Launder, B. E., and Tselepidakis, D. P., "Contribution to the Second-Moment Modelling of Sublayer Turbulent Transport," *Near-Wall Turbulence*, edited by S. J. Kline and N. H. Afgan, Hemisphere, New York, 1989, pp. 818–833.

[4]Daly, B. J., and Harlow, F. H., "Transport Equations in Turbulence," *Physics of Fluids*, Vol. 13, No. 11, 1970, pp. 2634–2649.

[5]Mansour, N. N., Kim, J., and Moin, P., "Reynolds-Stress and Dissipation-Rate Budgets in a Turbulent Channel Flow," *Journal of Fluid Mechanics*, Vol. 194, 1988, pp. 15–44.

[6]Kim, J., Moin, P., and Moser, R., "Turbulence Statistics in Fully Developed Channel Flow at Low Reynolds Number," *Journal of Fluid Mechanics*, Vol. 205, 1987, pp. 421–451.

[7]Spalart, P. R., "Direct Simulation of a Turbulent Boundary Layer up to $R_\theta = 1410$," *Journal of Fluid Mechanics*, Vol. 187, 1988, pp. 61–98.

[8]Launder, B. E., and Reynolds, W. C., "Asymptotic Near-Wall Stress Dissipation Rates in a Turbulent Flow," *Physics of Fluids*, Vol. 26, No. 5, 1983, pp. 1157, 1158.

[9]Hanjalic, K., "Advanced Turbulence Closure Models: A View of Current States and Future Prospects," *International Journal of Heat and Fluid Flow*, Vol. 15, No. 3, 1994, pp. 178–203.

[10]Djenidi, L., and Antonia, R. A., "Riblet Modelling Using a Second-Moment Closure," *Applied Scientific Research*, Vol. 54, No. 4, 1995, pp. 249–266.

[11]Launder, B. E., and Li, S. P., "On the Elimination of Wall Topography Parameters from Second-Moment Closure," *Physics of Fluids A*, Vol. 6, No. 2, 1994, pp. 999–1006.

[12]Reynolds, W. C., "Physical and Analytical Foundations, Concepts, and New Directions in Turbulence Modellings and Simulations," *Turbulence Models and Their Applications*, edited by B. E. Launder, W. C. Reynolds, W. Rodi, J. Mathieu, and D. Jeandel, Vol. 2, Collection de la Direction des Etudes et Recherches d'Electricité de France, Edition Eyrolles, Lyon, France, 1984, pp. 151–294.

[13]Durbin, P. A., and Speziale, C. G., "Local Anisotropy in Strained turbulence at High Reynolds Number," *Journal of Fluids Engineering*, Vol. 113, 1991, pp. 707–709.

[14]Antonia, R. A., Djenidi, L., and Spalart, P. R., "Anisotropy of the Dissipation Tensor in a Turbulent Boundary Layer," *Physics of Fluids*, Vol. 6, No. 7, 1994, pp. 2475–2479.

[15]Lai, Y. G., and So, R. M. C., "On the Near-Wall Turbulent Flow Modelling," *Journal of Fluid Mechanics*, Vol. 221, 1990, pp. 641–673.

[16]Lumley, J. L., and Newman, G. R., "The Return to Isotropy of Homogeneous Turbulence," *Journal of Fluid Mechanics*, Vol. 82, 1977, pp. 161–178.

[17]Antonia, R. A., Kim, J., and Browne, L. W. B., "Some Characteristics of Small Scale Turbulence in a Turbulent Duct Flow," *Journal of Fluid Mechanics*, Vol. 233, 1991, pp. 369–388.

[18]Hallbäck, M., Groth, J., and Johansson, A. V., "An Algebraic Model for Nonisotropic Turbulent Dissipation Rate in Reynolds Stress Closures," *Physics of Fluids A*, Vol. 2, No. 10, 1990, pp. 1859–1866.

[19]Tennekes, H., and Lumley, J. L., *A First Course in Turbulence*, MIT Press, Cambridge, MA, 1972.

[20]Lumley, J. L., *Prediction Methods for Turbulent Flows*, Lecture Series, Von Kármán Inst., Rhode-St-Genese, 1975.

[21]Rotta, J. C., "Statistichc Theorie Nichthomogener Turbulenz," *Zeitschrift fur Physik*, Vol. 129, 1951, pp. 547–572.

[22]Launder, B. E., Reece, G. J., and Rodi, W., "Progress in the Development of a Reynolds-Stress Turbulence Closure," *Journal of Fluid Mechanics*, Vol. 68, 1975, pp. 537–566.

[23]Launder, B. E., *A New Form of Second-Moment Closure: Introduction to the Modeling of Turbulence*, Lecture Series, Von Kármán Inst., Rhode-St-Genese, 1993.

[24]Schneider, G. E., and Zedan, M., "A Modified Strongly Implicit Procedure for the Numerical Solution of Field Problems," *Numerical Heat Transfer*, Vol. 4, 1981, pp. 1–19.

[25]Kawamura, H., "A k – ϵ – $\overline{v^2}$ Model with Special Relevance to the Near-Wall Turbulence," *Proceedings of the Eighth Symposium on Turbulent Shear Flows* (Munich), 1991, pp. 26.4.1–26.4.6.

[26]Launder, B. E., and Shima, N., "Second-Moment Closure for the Near-Wall Sublayer: Development and Application," *AIAA Journal*, Vol. 27, No. 10, 1989, pp. 1319–1325.

[27]Purtell, L. P., Klebanoff, P. S., and Buckley, F. T., "Turbulent Boundary Layer at Low Reynolds Number," *Physics of Fluids*, Vol. 24, No. 5, 1981, pp. 802–811.

[28]Ching, C. Y., Djenidi, L., and Antonia, R. A., "Low-Reynolds-Number Effects in a Turbulent Boundary Layer," *Experiments in Fluids*, Vol. 19, No. 1, 1995, pp. 61–68.

[29]Tavoularis, S., and Karnik, U., "Evolution of Stresses and Scales in Uniformly Sheared Turbulence," *Journal of Fluid Mechanics*, Vol. 204, 1989, pp. 457–478.

[30]Erm, L. P., "Low Reynolds Number Turbulent Boundary Layer," Ph.D. Thesis, Dept. of Mechanical Engineering, Univ. of Melbourne, Australia, Dec. 1988.

J. Kallinderis
Associate Editor